

The Role of the Nano/Microstructure in the Case of the Photodegradation of Two Model VOC Pollutants Using Commercial TiO₂

Giuseppina Cerrato^{1,*}, Claudia Letizia Bianchi², Sara Morandi¹, Carlo Pirola², Marta Stucchi², Maria Vittoria Diamanti³, Maria Pia Pedferri³, and Valentino Capucci⁴

¹*Dipartimento di Chimica and NIS, Center of Excellence, Università degli Studi di Torino, via P. Giuria 7, 10125 Torino, Italy, and Consorzio INSTM, via Giusti 9, 50121 Firenze, Italy*

²*Dipartimento di Chimica, Università degli Studi di Milano, via Golgi 19, 20133 Milano, Italy, and Consorzio INSTM, via Giusti 9, 50121 Firenze, Italy*

³*Dipartimento di Chimica, Materiali e Ingegneria Chimica "G. Natta", Politecnico di Milano, via Mancinelli 7, 20131 Milano, Italy, and Consorzio INSTM, via Giusti 9, 50121 Firenze, Italy*

⁴*Graniti Fiandre SpA, via Radici Nord 112, 42014 Castellarano, Italy*

Received: 1 March 2015

Accepted: 2 March 2015

1. INTRODUCTION

Since the early '70s heterogeneous photocatalysis has attracted a lot of interest: many different fields of application have been considered by the researchers, such as H₂ production, water purification, environmental abatement of both outdoor and indoor pollutants (such as volatile organic compounds—VOCs), etc.^{1–3}

A large amount of photocatalysts has been proposed and studied, but the most interesting system is represented by TiO₂, either bare or promoted/loaded by addition of transition/rare metal species.³

As far as water purification is pertained, quality and safety of water is a worldwide concern that is gradually becoming more important with increasing disruption of nature by human activities. Pollutants introduced in ground water include organic, inorganic, biological and radioactive contaminants produced from both natural and anthropogenic sources, almost all of which have human and environmental health concerns. For this reason,

global and national organisations such as the World Health Organisation (WHO) and the United States Environmental Protection Agency (US-EPA) set levels for pollutants in drinking water that have negative impacts on the health of the environment and those that live within it. However, it is often found that these levels are exceeded, especially in the developing countries, due to poor control of chemicals released into the environment, bad conditions of water supply networks, a misunderstanding of the future negative impact of pollutants or a lack of suitable remediation techniques.^{4–6}

Considering VOCs, it is well known that they are emitted in the troposphere by both anthropogenic and biogenic sources;⁷ moreover, they can be present in either outdoor or indoor environments (offices, schools, houses, etc.) and may form as such or as by-products/degradation products of heavier molecules.⁸ Among the many VOCs that can be present in indoor locations, both aromatic and aliphatic compounds can exist: for example, benzene, toluene, ethylbenzene and o-xylene (BTEX) are well known pollutants that can accumulate indoor.⁹ Their abatement from gas-phase has been extensively studied employing TiO₂-based materials,¹⁰ focusing in particular on the relationship

*Author to whom correspondence should be addressed.

Email: giuseppina.cerrato@unito.it

between TiO₂ surface species and the consequent catalytic efficiency.¹¹

Nevertheless, while for outdoor pollution several international regulations are in force to limit the hazard for human health and the environment, no restriction is currently available for indoor contaminants. However, there are clear guidelines that indicate limit threshold values for specific pollutants, for instance those indicated in USA¹² and EU reports.¹³

TiO₂-based materials present several attractions for both the degradation set-up and the economy of the pathway:

- (i) the catalyst is almost inexpensive,
- (ii) operations are carried out at ambient temperature,
- (iii) the final by-products are usually CO₂ and H₂O,
- (iv) no other chemical reagent is needed.

Nevertheless, particular attention has to be paid to the size of the particles the catalyst is made of: in fact, even if few specific restrictions are present in this respect, several studies have already evidenced the negative impact of nanoparticles on human health (Ref. [14 and references therein]). For these reasons, in the present paper we focused our attention onto the photodegradation in gas-phase of two different pollutants, namely isopropanol and acetone, employing

- (i) a series of commercial TiO₂ powders whose target market is not photocatalysis and
- (ii) a reference nano-sized TiO₂ powder by Evonik (P25) specifically targeted for photocatalytic applications, and comparing their behaviour on the basis of the obtained results.

The two pollutants were accurately chosen because acetone is also one of the by-products coming from the photodegradation pathway of isopropanol and thus its investigation can give precise information on the final steps of the mineralization of the mother-molecule.

2. EXPERIMENTAL DETAILS

2.1. Materials

Five commercial TiO₂ materials by Kronos, Huntsman, Sachtleben (two different powders) and Cristal (which will be respectively quoted with the A–E letters in the following), all available in the market as pigmentary powders, have been selected with the following features: pure anatase phase, uncoated surface, undoped material, not sold as photocatalytic material. P25 by Evonik was chosen as nano-sized reference material for its peculiar photocatalytic characteristics. All commercial powders were used as received without any further treatment or activation process.

2.2. Methods

The specific surface area (SSA) of all samples was determined by N₂ adsorption/desorption experiments at 77 K

(BET method) using a Sorptometer instrument (Costech Mod. 1042).

The crystalline nature of the samples was investigated by X-ray diffraction (XRD) using a PW3830/3020 X'Pert diffractometer from PANalytical working in a Bragg-Brentano geometry, using the Cu K_{α1} radiation ($\lambda = 1.5406 \text{ \AA}$). The calculation of crystallite size was performed by applying the Scherrer equation:

$$D = 0.9 \cdot \lambda / (\beta_{\text{hkl}} \cdot \cos \theta_{\text{hkl}})$$

where D is the crystallite size, λ is the X-ray wavelength of radiation for CuK α , β_{hkl} is the full-width at half maximum (FWHM) at (hkl) peak and θ_{hkl} is the diffraction angle.

The morphology of the catalysts was inspected by means of high-resolution electron transmission microscopy (HR-TEM) using a JEOL 3010-UHR instrument (acceleration potential: 300 kV; LaB₆ filament). Samples were “dry” dispersed on lacey carbon Cu grids.

X-ray photoelectron spectra (XPS) were collected in an M-probe apparatus (Surface Science Instruments). The source was monochromatic Al K α radiation (1486.6 eV).

Contact angle measurements were performed on the as-received powders and after their irradiation for 3 h under UV-A lamp in order to verify on all samples the presence or absence of the super-hydrophilic nature, one of the more interesting properties of a photocatalytic material.

2.3. Photocatalytic Tests

The photocatalytic activity of all samples was tested in the gas-phase degradation of both isopropanol and acetone. In the former case, specimens were prepared by depositing a water-TiO₂ slurry on a flat glass slide, followed by oven drying at 70 °C for 4 h; the amount of catalyst deposited ranged from 0.5 mg to 0.7 mg, distributed on an area of approximately 250 mm². Three specimens for each TiO₂ powder were produced and tested for isopropanol photocatalytic degradation in batch conditions. Each specimen was placed in a 100 ml glass reactor with quartz window, inside which 1 ml of air saturated with isopropanol was injected; the final isopropanol concentration in cell was estimated to be approximately 2 ppmv. Irradiation was provided by a 300 W UV-Vis lamp (Osram Vitalux) with intensity of 15 Wm⁻² in the UV-A wavelength range, and lasted for 3 h. Degradation of isopropanol was followed by repeated gas chromatography (GC) analyses; to exclude absorption or leakage as sources of isopropanol disappearance, its degradation was verified by observing the formation of its primary by-product, i.e., acetone, as described in detail elsewhere.¹⁵

As acetone is one of the by-products of the isopropanol photodegradation, its abatement was followed in batch conditions in a more suitable way. The setup was precisely described elsewhere.^{14a, 16} Photocatalytic degradations were conducted in a Pyrex glass cylindrical reactor

with diameter of 200 mm and effective volume of 5 L. The amount of catalyst (in the form of powder deposited from 2-propanol slurry on flat glass disks) used in the tests was 0.05 g.¹⁷ The gaseous mixture in the reactor was obtained by mixing hot chromatographic air, humidified at 40%, and a fixed amount of volatilized pollutant, in order to avoid condensation. The initial concentration of VOCs in the reactor was deliberately increased at a very high value, 400 ppmv, in order to verify the TiO₂ performance even in very stressing conditions. Photon sources were provided by a 500 W iron halogenide lamp (Jelosil, model HG 500) emitting in the UV-A range at 30 Wm⁻². Acetone tests lasted 3 h, and the actual concentration of pollutant in the reactor was determined directly by micro-GC sampling.

3. RESULTS AND DISCUSSION

3.1. Physico-Chemical Characterisation of the Powders

A thorough physico-chemical characterisation of all the quoted samples has been carried out and reported elsewhere.¹⁸ However, the main features of all materials have been summarised in Table I, in which it is possible to observe that a residual, appreciable percentage of rutile phase is present only in the case of the reference P25 powder, exhibiting all the other TiO₂ samples only the anatase phase. As for the mean dimensions of the crystallites, the Scherrer equation was applied to the (101) planes reflection, corresponding to the $2\theta = 25.5^\circ$ diffraction peak: a good agreement between these indications, the values of specific surface area (both listed in Table I) and the morphological features observed by means of HRTEM analyses (reported in Fig. 1), is evident in particular for A, B and E materials. On the other hand, P25 but also sample C present a nanometric nature, exhibiting crystals size of about 25 and 40 nm, respectively, that accounts for their higher specific surface area. Only in the case of sample D, it was not possible to perform calculations owing to the co-presence of nano and micro-sized crystallites, confirmed by HRTEM investigations.¹⁸

The surface chemical states of TiO₂ particles have been analysed by XPS. No appreciable differences can be singled out in the Ti 2p region among all samples

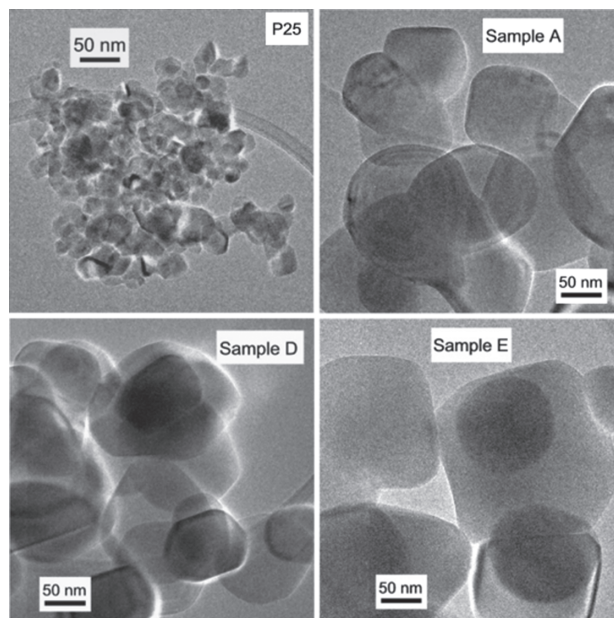


Fig. 1. HRTEM images: the name of the sample is indicated in each section.

concerning the binding energies (BE) and the full width at half-maximum (FWHM) values (not reported). The peak of Ti 2p_{3/2} is always regular and its BE at about 458.4 eV agrees well with the data for Ti(IV) in TiO₂ materials.^{19,20}

3.2. Photo-Degradation of the Pollutants

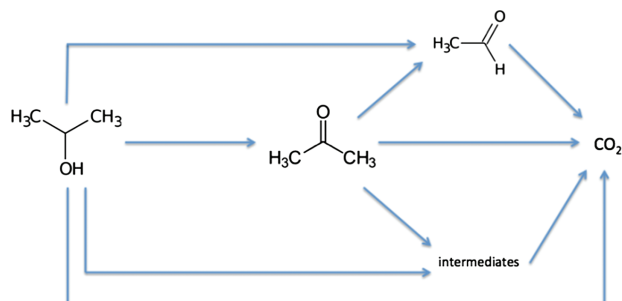
Two different test molecules have been considered as specific probes representing indoor pollution, i.e., isopropanol and acetone. In particular, the latter is also present as intermediate in the degradation pathway of isopropanol:¹⁵ see Scheme 1.

Moreover, acetone is itself an important pollution source in indoor environment and its own photodegradation kinetics cannot be carefully studied in isopropanol degradation tests. Therefore, the evaluation of this second reaction comes in cascade to fully characterize the degradation reactions occurring from isopropanol to acetone to full degradation.

A general starting consideration is necessary about the possible adsorption of both pollutant model molecules

Table I. Main features of the various TiO₂ powders.

Sample	Anatase: rutile	Average crystallite size (nm)	SSA (m ² /g)	XPS	OH/O _{TOT} (XPS)
P25	75:25	26	50	Ti(IV)	0.14
A	100	105	12	Ti(IV)	0.32
B	100	95	11	Ti(IV)	0.12
C	100	40	23	Ti(IV)	0.11
D	100	Mix (micro-sized+ ultrafine)	11	Ti(IV)	0.27
E	100	180	11	Ti(IV)	0.24



Scheme 1. Degradation pathway for isopropanol.

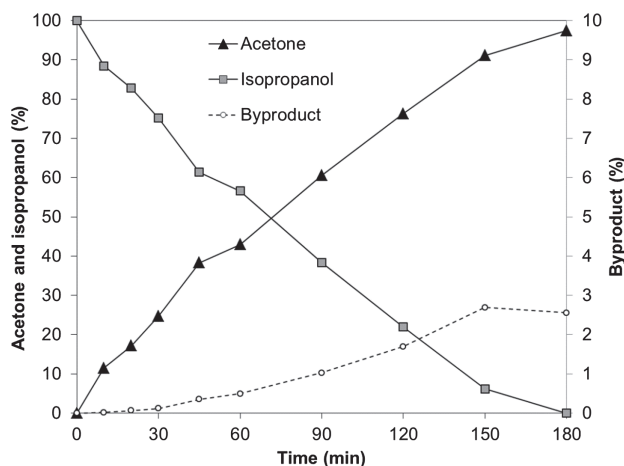


Fig. 2. Trend of pollutants concentration in cell atmosphere as a function of irradiation time for the reference P25 powder.

onto TiO_2 particles: in both cases blank tests were carried out in the same experimental conditions but in the absence of UV irradiation, leading to a negligible adsorption.

As for isopropanol degradation, a first example of test results related to P25 is reported in Figure 2. Data are presented in form of percentage, which was calculated by converting GC peak areas into concentration values. GC revealed the gradual reduction of the isopropanol peak to its complete abatement, with the concurrent formation of a small secondary peak, increasing in magnitude with irradiation time that was associated with acetone formation. After acetone appearance, a third peak, of smaller intensity, was also noticed to form, which in turn was associated with a non-identified acetone degradation by-product (subsequently identified as acetaldehyde in the second photodegradation set of tests performed with the second experimental set-up). At the end of the reaction, all the isopropanol was completely degraded and a 10% of acetone was still present in the gas phase together with the third species. The same trend, with different rates of isopropanol decomposition, was observed in all tests carried out with all TiO_2 powders examined.

Figure 3 presents a comparison among degradation efficiencies of isopropanol, calculated as the complementary to 100% of isopropanol concentration in the reactor atmosphere, in the presence of the different TiO_2 powders tested. Data presented were calculated as the mean values of different tests performed on specimens prepared in identical conditions. Results indicate the obtaining of higher photocatalytic efficiency in the case of powder B, closely followed by A; specimens C, and similarly D, show slightly slower isopropanol degradation, close to that observed in the case of the reference samples of P25. Finally, powder E exhibited a net reduction of photocatalytic efficiency: only in this case 100% isopropanol degradation was not reached within the 3 h of test.

Acetone is a very interesting molecule from the degradation point of view because it is a by-product of the

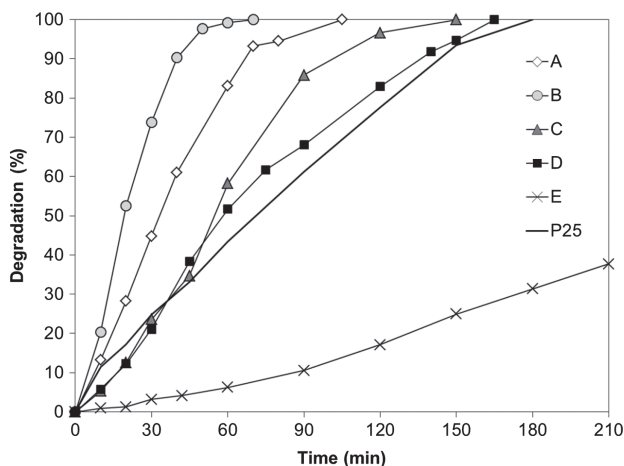


Fig. 3. Degradation extent of isopropanol in the presence of different photocatalysts as a function of irradiation time.

degradation of isopropanol, as previously confirmed. Moreover, its reaction pathway passes through the formation of acetaldehyde as reported by Stengl et al.¹⁶ and confirmed by a previous paper by the authors:¹⁴ see Scheme 1.

Notwithstanding the high pollutant concentration inside the reactor, the nano-sized P25 and C samples exhibited high photocatalytic efficiency (see Fig. 4), leading to the complete pollutant degradation within shorter reaction time (less than 80 min) compared to the micro-sized materials. Nevertheless, a very interesting behaviour was observed for sample D (see Fig. 4), characterized by a micro-sized nature with the co-presence of a fraction of nano-sized particles which exhibited very fast acetone degradation with the complete disappearance of the pollutant after 60 min (*vide infra*).

Except for E sample, the only by-product of the reaction was carbon dioxide, confirming the complete degradation of both acetone and acetaldehyde without formation

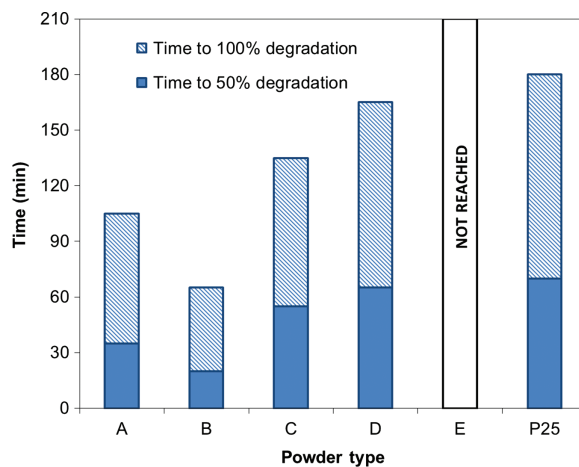


Fig. 4. Summary of degradation extent reached by the powders tested: emphasis is given to the time required to reach either 50% and 100% degradation of the quantity of pollutant present in the cell.

of adsorbed by-products on the samples surface: the latter feature was verified by FTIR measurements on the sample surface after the kinetic runs (data not reported). A different behaviour was shown by sample E, which exhibited an incomplete degradation of acetone after 2 h of tests. Interestingly, despite the low surface area, the micro-sized samples A and B showed the complete pollutant degradation, with an increase in the time required to reach 100% degradation of only 15–30% compared to P25.

The high photocatalytic activity of TiO₂ samples was put in correlation with the surface OH concentration detected by XPS measurements^{14a} and reported in the sixth column of Table I. In fact, the high OH concentration at the surface can favor the adsorption of pollutants (and intermediates of degradation as well), thus leading to a very active photocatalyst.

However, considering only OH/O_{TOT} ratio, the catalytic results presents some discrepancies. For example, micro-sized samples A and B have higher hydrophilicity/hydrophobicity ratio than P25 but lower catalytic efficiency in the case of acetone degradation. On the other hand, considering surface area and particle size (see Table I), acetone photodegradation follows the trend: the smaller is the crystallite size, the faster is the photocatalytic reaction kinetics, with an interesting discrepancy for sample D, characterized by the co-presence of both nano and micro-sized crystallites.

If we try to summarize the photodegradation results in order to obtain “absolute” data (obtained dividing the photodegradation % taken after 1 hour of reaction by the SSA of each powder) for all the quoted samples, we obtain the data reported in Table II. It is evident that for both A and B powders the highest efficiency per unit specific surface area has been reached, being B the best sample among all, C and D exhibit intermediate values, being D the best between the two, whereas E exhibits the lowest specific efficiency, as well as, unexpectedly, the reference nano-sized TiO₂, i.e., P25.

The super-hydrophilic nature of all materials was verified by contact angle measurements performed on the as-received samples and on the same irradiated for 3 h under UV-A lamp. In Figure 5, the results obtained for P25 and sample B are reported (the results obtained for plain glass have been reported as a reference). The pristine nanometric sample exhibits a lower contact angle (10°) than all the

Table II. Absolute degradation values for the various TiO₂ powders.

Sample	SSA (m ² /g)	% degradation after 1 hour of reaction (from Fig. 3)	% degradation/SSA
P25	50	42	0.84
A	12	83	6.91
B	11	99	9.00
C	23	57	2.48
D	11	51	4.63
E	11	6	0.55

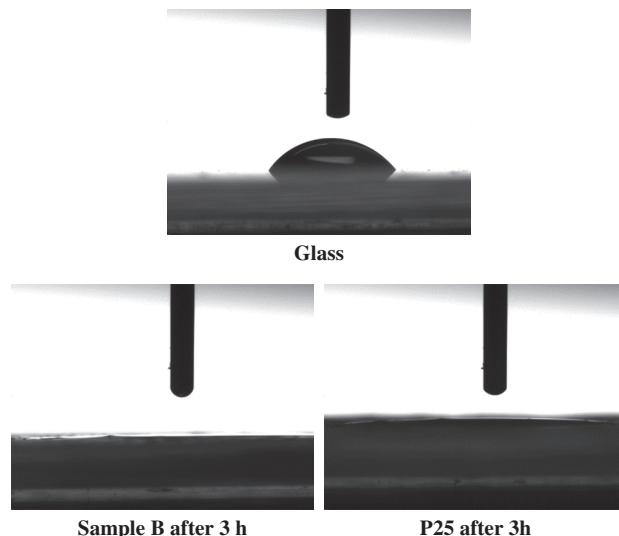


Fig. 5. Contact angle measurements for sample B (left-hand section) and P25 (right-hand section) materials (glass has been reported for comparison purposes: see top section).

other samples (average values 20° ± 5°). After 2 h irradiation, all samples show a super-hydrophilic behavior with a non measurable angle being less than 1°.

4. CONCLUSIONS

The present article compares the photocatalytic performances of five commercial TiO₂ powders with those of the reference P25 system, in the degradation of two important VOCs, isopropanol and acetone, representative of indoor pollution.

The different performances achieved by the various materials are representative of the very different physico-chemical features exhibited by all of them. If a trend can be put into evidence, it is most likely to be related to the correct ratio between the value of specific surface area and the hydrophilicity (hydrophobicity) possessed by the commercial powders with respect to that shown by the P25 reference system.

Last but not least, it is worth noting that the present research indicated that also micro-sized TiO₂ powders, of commercial origin and normally employed as pigments, are very promising materials to be used in the photocatalytic degradation of indoor VOCs, such as isopropanol and acetone, which would help limiting the risks for human health deriving from the use of nanoparticles.

References and Notes

- M. R. Hoffman, S. T. Martin, W. Y. Choi, and D. W. Bahnemann, *Chem. Rev.* **95**, 69 (1995).
- A. Fujishima, T. N. Rao, and D. A. Tryk, *J. Photochem. Photobiol. C* **1**, 1 (2000).
- A. Di Paola, E. Garcia-Lopez, G. Marci, and L. Palmisano, *J. Hazard. Mater.* **211**, 3 (2012).

4. C. Reimann, K. Bjorvatn, B. Frengstad, Z. Melaku, R. Tekle-Haimanot, and U. Siewers, *Sci. Total Environ.* 311, 65 (2003).
5. M. A. H. Bhuiyan, M. A. Islam, S. B. Dampare, L. Parvez, and S. Suzuki, *J. Hazard. Mater.* 179, 1065 (2010).
6. S. Karavoltzos, A. Sakellari, N. Mihopoulos, M. Dassenakis, and M. J. Scoullou, *Desalination* 224, 317 (2008).
7. R. Atkinson and J. Arey, *Chem. Rev.* 103, 4605 (2003).
8. J. Roberts and W. C. Nelson, National Human Activity Pattern Survey Data Base, United States Environmental Protection Agency (USEPA), Research Triangle Park, NC (1995).
9. (a) Institute for Environment and Health (IEH). IEH assessment on indoor air quality in the home. Institute for Environment and Health, Leicester, UK (1996); (b) NIOSH CIB 63, DHHS (NIOSH) Publication No. 2011-160.
10. C. H. Ao, S. C. Lee, C. L. Mak, and L. Y. Chan, *Appl. Catal. B, Environmental* 42, 119 (2003).
11. S. Ardizzone, C. L. Bianchi, G. Cappelletti, A. Naldoni, and C. Pirola, *ES&T* 42, 6671 (2008).
12. Y. S. Lee and D. A. Guerin, *Building and Environment* 45, 1104 (2010).
13. http://ihcp.jrc.ec.europa.eu/our_activities/public-health/indoor_air_quality/indoor-air-quality-jrc-contribution-to-guidelines.
14. (a) C.L. Bianchi, S. Gatto, C. Pirola, A. Naldoni, A. D. Michele, G. Cerrato, V. Crocellà, and V. Capucci, *Appl. Catal. B: Environmental* 146, 123 (2014); (b) H. M. Braakhuis, M. V. D. Z. Park, I. Gosens, W. H. De Jong, and F. R. Cassee, *Particle and Fibre Toxicology* 18, 11 (2014).
15. M. V. Diamanti, M. Ormellese, and M. P. Pedferri, *Cem. Concrete Res.* 38, 1349 (2008).
16. V. Stengl, V. Houskova, S. Bakardjieva, and N. Murafa, *New J. Chem.* 34, 1999 (2010).
17. C. L. Bianchi, C. Pirola, E. Selli, and S. Biella, *J. Haz. Mater.* 211, 203 (2012).
18. C. L. Bianchi, C. Pirola, F. Galli, G. Cerrato, S. Morandi, and V. Capucci, *Chem. Eng. J.* 261, 76 (2015).
19. G. Cappelletti, C. L. Bianchi, and S. Ardizzone, *Appl. Surf. Sci.* 253, 519 (2006).
20. S. Ardizzone, C. L. Bianchi, G. Cappelletti, S. Gialanella, C. Pirola, and V. Ragaini, *J. Phys. Chem. C* 111, 13222 (2007).